Fatigue crack paths under the influence of changes in stiffness

G. Kullmer, B. Schramm, H. A. Richard
Paderborn University, Germany
kullmer@fam.upb.de

ABSTRACT. An important topic of the Collaborative Research Centre TRR 30 of the Deutsche Forschungsgemeinschaft (DFG) is the crack growth behaviour in graded materials. In addition, the growth of cracks in the neighbourhood of regions and through regions with different material properties belongs under this topic. Due to the different material properties, regions with differing stiffness compared to the base material may arise. Regions with differing stiffness also arise from ribs, grooves or boreholes. Since secure findings on the propagation behaviour of fatigue cracks are essential for the evaluation of the safety of components and structures, the growth of cracks near changes in stiffness has to be considered, too. Depending on the way a crack penetrates the zone of influence of such a change in stiffness and depending on whether this region is more compliant or stiffer than the surrounding area the crack may grow towards or away from this region. Both cases result in curved crack paths that cannot be explained only by the global loading situation. To evaluate the influence of regions with differing stiffness on the path of fatigue cracks the paths and the stress intensity factors of cracks growing near and through regions with differing stiffness are numerically determined with the program system ADAPCRACK3D. Therefore, arrangements of changes in stiffness modelled as material inclusions with stiffness properties different from the base material or modelled as ribs and grooves are systematically varied to develop basic conclusions about the crack growth behaviour near and through changes in stiffness.

KEYWORDS. Curved crack path; Crack growth simulation; Material inclusion; Change in stiffness; Finite elements.

INTRODUCTION

An important topic of the Collaborative Research Centre TRR 30 of the Deutsche Forschungsgemeinschaft (DFG) is the crack propagation behaviour in graded materials. In addition, the growth of cracks in the neighbourhood of material boundaries belongs under this topic. In particular, accidentally embedded extraneous material causes material boundaries. In many cases, material inclusions represent regions with stiffness properties different from the base material and the boundaries of these regions represent local changes in stiffness. Furthermore, ribs, grooves or boreholes cause similar changes in stiffness. Depending on the way a crack penetrates the zone of influence of a region with different stiffness and depending on whether this region is more compliant or stiffer than the surrounding area the crack may grow towards or may tend to grow away from the change in stiffness. If the crack crosses the change in stiffness, the crack growth behaviour reverses. If the region with different stiffness is locally bordered, the crack may grow around this region. All mentioned cases result in curved crack paths. Curved crack paths result from mixed mode loading at the crack tip. Thereby in general the basic crack opening modes co-occur, see Fig. 1. Mode I describes normal loading leading to a

symmetrical opening of the crack surfaces. Mode II is valid for shear loading causing in-plane sliding of the crack surfaces. Mode III represents shear loading generating anti-plane sliding of the crack surfaces.
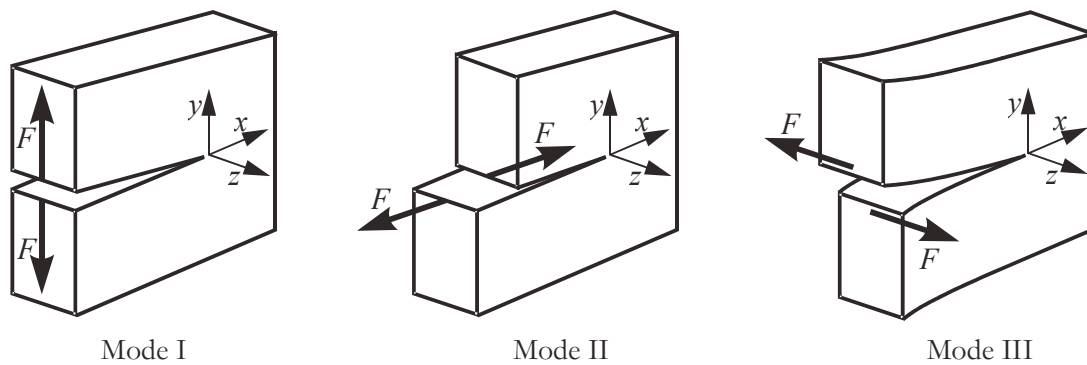

Figure 1: Basic crack opening modes, Richard and Sander [1].

Since the present study only deals with plane problems, mode III is irrelevant. Whereas a crack propagates self-similar under mode I-loading it deflects under mode II-loading about the angle $\varphi_0 \approx 70°$ as represented in Fig. 2. Under plane mixed-mode-loading with continuously changing ratios of mode I and mode II curved cracks form in the x-y-plane according to Fig. 1.
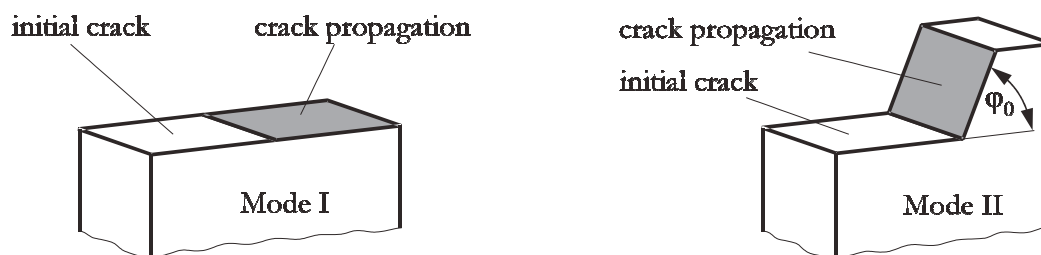

Figure 2: Crack propagation under different crack opening modes, Richard and Sander [1]

SIMULATION MODEL FOR THE INVESTIGATION OF THE FATIGUE CRACK GROWTH IN THE NEIGHBOURHOOD OF CHANGES IN STIFFNESS

Simulation models based on the CT-specimen, see Fig. 3, are used to investigate the basic influence of line-shaped regions with differing stiffness and different orientation on the path of fatigue cracks. The default thickness of the specimen is 5mm and the default value of Young´s modulus is 210.000MPa. The material behaviour is idealised as linear elastic, isotropic and homogeneous. Poisson´s ratio is zeroed to avoid stresses in thickness direction of the specimen and thickness influences and therefore to ensure a state of plane stress in spite of using a three-dimensional model. A three-dimensional model is required for the present investigation since the crack growth is simulated with the program system ADAPCRACK3D developed by the Institute of Applied Mechanics of the University of Paderborn (Fulland [2]).

As shown in Fig. 3 a rectangular partition inserted into the CAD-model of the CT-specimen represents the line-shaped region with differing stiffness. The simulation models differ since Young´s modulus, the thickness, the distance to the starter notch and the orientation of the line-shaped change in stiffness vary. To evaluate the influence of the stiffness mismatch, on the one hand, with default thickness Young´s modulus of the line-shaped region is varied and on the other hand, with standard Young´s modulus the thickness of the line-shaped region is modified. To analyse the influence of the orientation of the change in stiffness in relation to the nominal global mode I-loading of the initial crack, the orientation of the change in stiffness is varied by stepwise rotation of the line-shaped region about the centre A. Thus, for a fixed distance d = 9.7mm the orientation angle α varies between 90° and 30°. To investigate the influence of the distance d between the starter notch and the change in stiffness with default thickness and constant orientation angle α = 45° the distance d varies in steps of 2.5mm from 9.7mm to 19.7mm. For this investigation, Young´s modulus of the line-shaped region is once double and once half the value of default Young´s modulus.
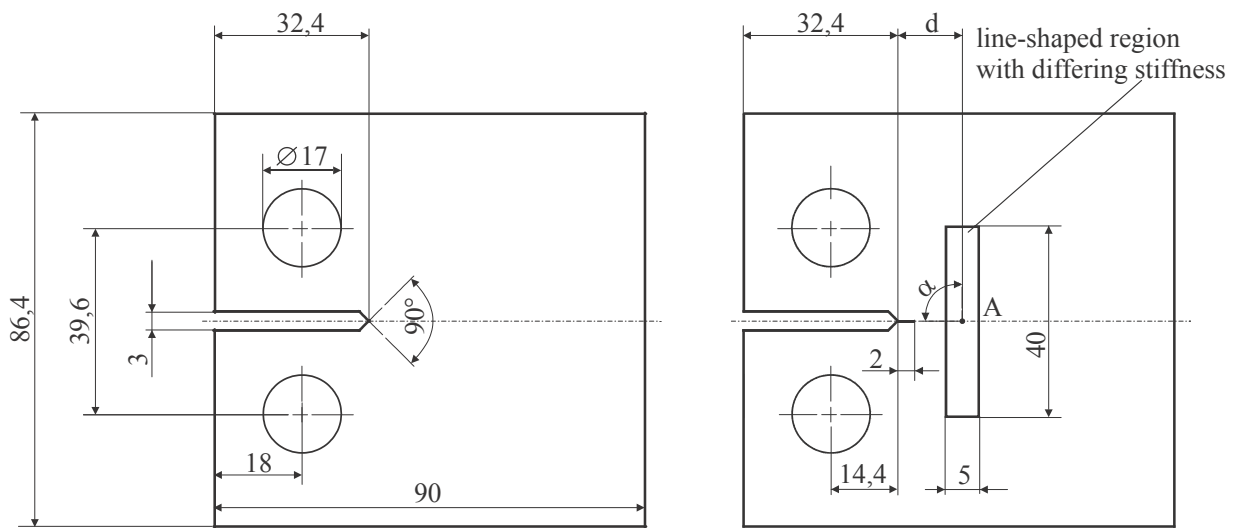
Figure 3: Geometry of the CT-specimen and positioning of the line-shaped region with differing stiffness.

The CT-specimen is partitioned according to Fig. 4. Inside the partitions P1 and P2, the default properties of Young´s modulus and the thickness of the specimen are valid. Whereas inside partition P3, that represents the region with differing stiffness, depending on the type of examination either Young´s modulus or the thickness varies. The partition P2 guarantees a comparable fine mesh in the neighbourhood of the partition P3 and identical boundary conditions independent from the orientation angle α and the distance d of the change in stiffness. Therefore, the border of partition P2 is sufficiently distant from the partition P3 for all investigated orientations and positions of the change in stiffness.

Furthermore, Fig. 4 shows the boundary conditions. All simulation models are supported at the positions A, B and C. The bearing is statically determined and symmetrical. The specimen is loaded with distributed line loads of 2500N/mm at the upper and lower inner side of the bore. With a specimen thickness of 5mm the resulting load is 12.5kN. The boundary conditions are chosen in a way that the bearing reactions vanish and a symmetrical deformation of the specimen occurs if all partitions of the specimen have the same Young´s modulus and the same thickness. In this case, a pure mode I-loading is present at the crack tip and the crack should grow straight ahead.
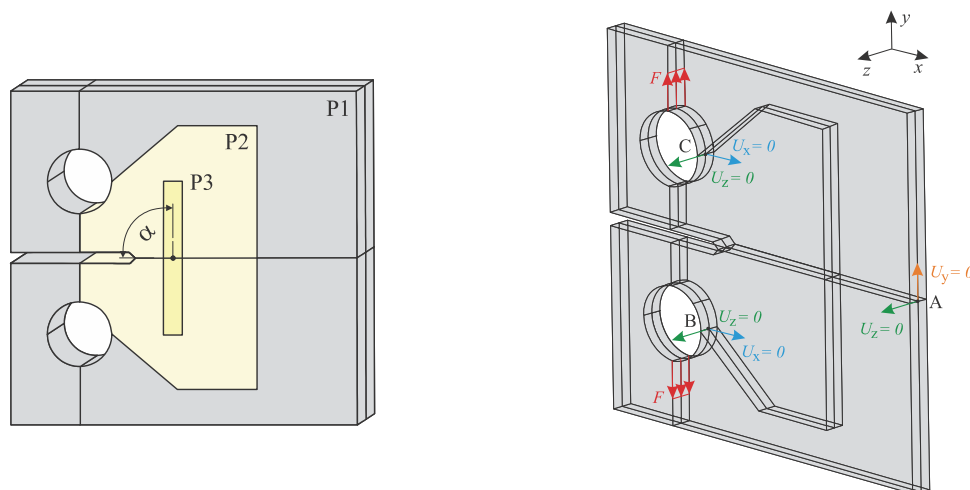

Figure 4: Partitioning of the CT-specimen and definition of the boundary conditions.

Fig. 5 shows a typical global mesh exemplary for the CT-specimen with a change in stiffness with an orientation angle α = 45°. The mesh consists of 10-noded quadratic tetrahedral elements. Inside the partitions P2 and P3 where the crack most likely will propagate the edge length of the elements is chosen 1mm whereas in partition P1 an edge length of 2.5mm is sufficient.
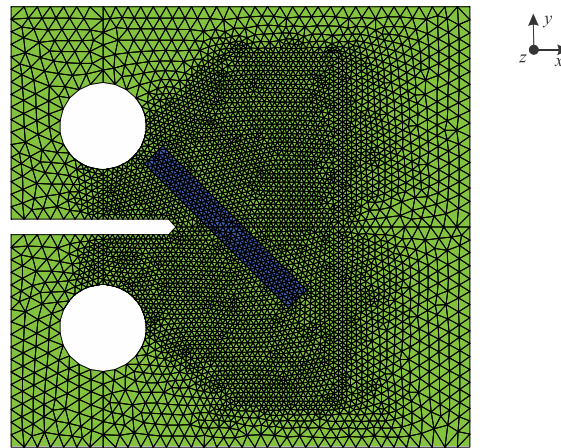
Figure 5: Exemplary mesh for the CT-specimen with a change in stiffness, orientation angle of the change in stiffness α = 45°.

For the crack growth simulation with ADAPCRACK3D the global mesh is unstitched along the crack path with the aid of a crack model. The crack model is a surface mesh that contains only the surface of the crack. At first, the crack model is built up of the mesh of the initial crack as shown in Fig. 6. Therefore, linear triangle elements with an edge length of 0.5mm are used. The initial crack has a lateral length of 2mm as defined in Fig. 3. For a growing crack, the crack model is incrementally extended with additional crack surfaces in the direction depending on the estimated mixed mode ratio. Since, as already mentioned, the present investigation in principle represents a plane problem, Poisson´s ratio is zeroed to ensure a state of plane stress and the stress intensity factor K_{III} is neglected to avoid a twisting of the crack surface. Furthermore, ADAPCRACK3D is modified in a way that with every simulation step a uniform crack increment over the specimen thickness with a fixed lateral length is achieved. Additionally it is meaningful to use the mapped mesh-method to mesh the initial crack as shown in Fig. 6 to achieve constant crack deflection angles, because ADAPCRACK3D uses local coordinate systems based on the mesh of the previous crack surface to calculate the coordinates of the new crack front nodes.
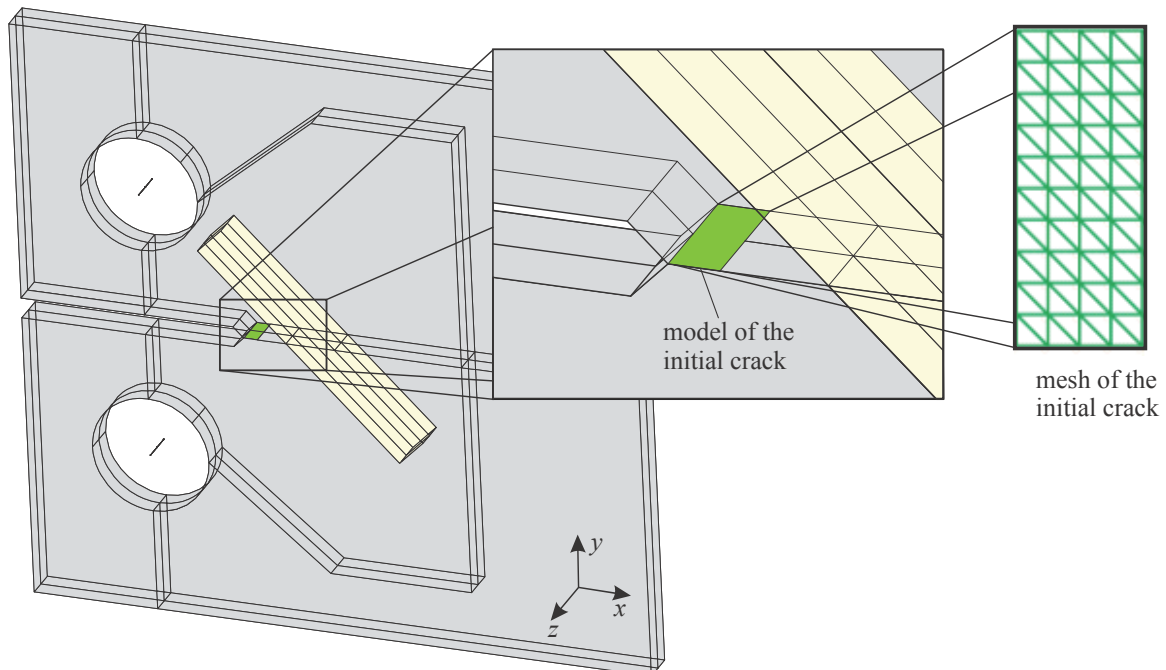

Figure 6: Positioning of the crack model inside the CT-specimen, orientation angle of the change in stiffness α = 45°.

For the calculation of the stress intensity factors K_I und K_{II} ADAPCRACK3D uses the modified virtual crack closure integral (MVCCI) after Rybicki and Kanninen [3] applied to a comoving submodel composed of a regular linear

hexahedral mesh containing the crack front. Thereby for every node at the crack front, first the energy release rates G_I and G_{II} for the respective crack opening modes are calculated. To evaluate the stress intensity factors K_I and K_{II} the mean values of the energy release rates G_I and G_{II} over the thickness of the specimen and the equations valid for the state of plane stress

$$K_I = \sqrt{G_I E} \tag{1}$$

$$K_{II} = \sqrt{G_{II} E} \tag{2}$$

are used. Since plane mixed mode loading is existent, the crack deflection angles are calculated with the maximum tangential stress criterion after Erdogan and Sih [4].

VERIFICATION OF THE CRACK GROWTH SIMULATIONS

Before the execution of the actual numerical simulations of CT-specimens with different changes in stiffness, the simulation model and the modified version of ADAPCRACK3D are verified. Therefore, simulations with the intended different values of Young´s modulus, the different thicknesses and a constant orientation angle $\alpha = 90°$ are conducted. Due to symmetry mode II should be zero and the crack should grow straight through the changes in stiffness independent of Young´s modulus or the thickness of the change in stiffness. The numerically determined resulting crack paths for all cases are almost straight with slight deviations from zero in y-direction. The extent of the deviations is for the CT-specimen with a homogeneous partition P3 with default Young´s modulus and default thickness as big as for the CT-specimens with different changes in stiffness. Already numerical inaccuracies due to an asymmetric FE-mesh, typical for using the free mesh option, cause slight deviations from a straight crack path. The maximum deviation from the straight line is in all cases for a simulated additional crack length of more than 20mm less than 0.2mm. Thus, the simulation model and the modified version of ADAPCRACK3D are suitable for the intended investigation.

Moreover, crack growth simulations with the CT-specimen with a change in stiffness with Young´s modulus double the default Young´s modulus and an orientation angle $\alpha = 45°$ are executed with crack growth increments of 0.2mm, 0.5mm und 1mm. Because the resulting crack paths are almost the same, the fixed default crack increment of 0.5mm for the further simulations is chosen, since this uniform crack increment has turned out to be a reasonable compromise between effort and accuracy.

CRACK PATHS FOR DIFFERENT ORIENTATIONS OF AN INCLUSION

The simulated crack paths for different orientations angles of a change in stiffness modelled as an inclusion and the alignment of the inclusion for the extreme orientation angles $\alpha = 30°$ as well as $\alpha = 90°$ are presented in Fig. 7. For the stiff inclusion, Young´s modulus is double the default Young´s modulus and for the compliant inclusion, Young´s modulus is half the default Young´s modulus.
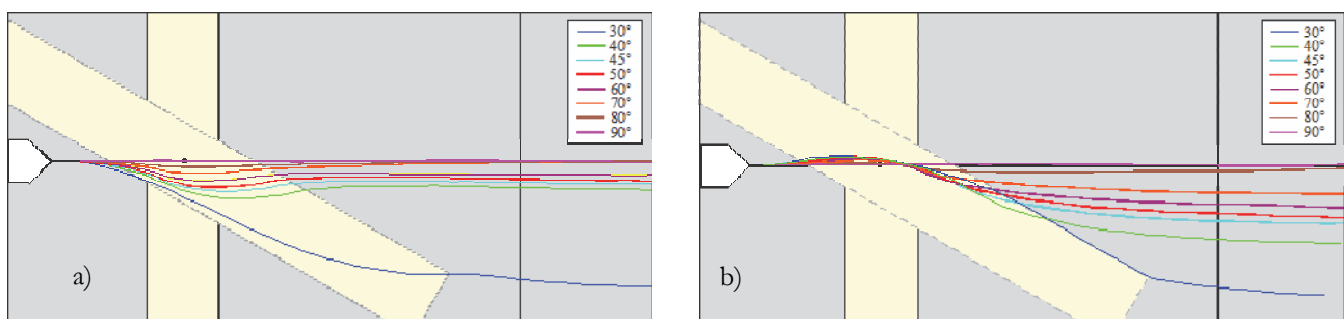

Figure 7: Simulated crack paths with variable orientation of the inclusion, a) stiff inclusion, b) compliant inclusion.

For α = 90° the crack propagates independently of the inclusion stiffness straight through the inclusion. With increasing inclination angle of the inclusion, the deflection of the crack rises. If the crack penetrates the region influenced by the stiffness mismatch of an inclined inclusion the crack tends to grow around the boundary to the stiff material and to grow towards the boundary to the compliant material. This can be clearly seen with the simulation results for the inclusion with orientation angle α = 30°. In this case, the crack hardly enters the stiff inclusion. Furthermore, the crack grows along the boundary of the compliant inclusion and leaves the inclusion at the farthest corner. In both cases the orientation angle α = 30° seems to be a lower limit so that the crack properly traverses the inclusion. If the crack traverses the inclusion the crack growth behaviour reverses approaching the second material boundary. When the crack leaves the region influenced by the stiffness mismatch the crack approaches tangentially a parallel to the extension line of the initial crack. The offset of the parallel to the extension line increases with the inclination of the inclusion. Where the crack crosses a material boundary, the crack path has an inflexion point and the curvature of the crack path changes. This means that the stress intensity factor K_{II} is zero at the material boundary and the crack locally grows straight under mode I conditions. The maximal magnitude of K_{II} corresponds with the maximal curvature of the crack path and the maximal stiffness asymmetry around the crack tip due to the inclusion. Anyway, K_{II} is small compared to K_I leading to slightly curved crack paths.

CRACK PATHS FOR STIFF CHANGES IN STIFFNESS

Fig. 7 shows crack paths through changes in stiffness due to doubling or halving Young´s modulus in partition P3. These results are already discussed in [5, 6]. Fig. 8 presents the comparison between crack paths due to changes in stiffness with double Young´s modulus or double thickness for the orientation angles α = 45° and α = 60°.
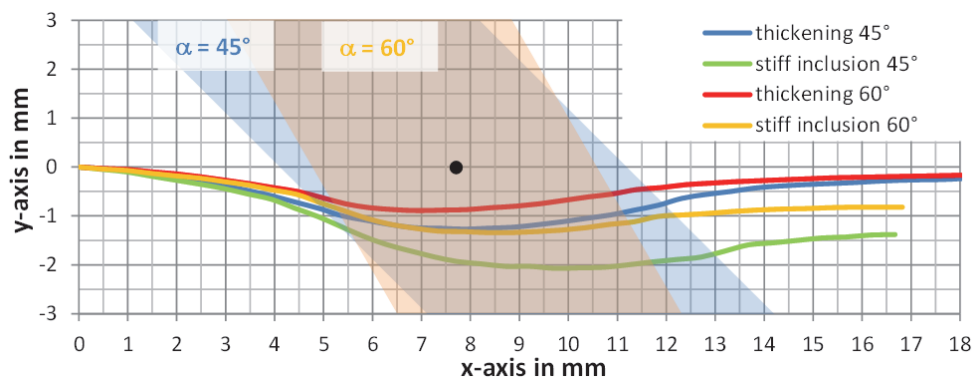

Figure 8: Crack paths for different orientation angles of stiffenings

The comparison of crack paths in Fig. 8 shows that in the neighbourhood of different kinds of stiffenings the principle characteristics of the crack paths are similar. If the crack enters the region of influence of a stiffening, the crack grows away from the stiffening. With increasing inclination of the stiffening, the deflection of the crack rises with the tendency that the crack tangentially passes by this region, see Fig. 7. If the extent of the stiffening is too big or the inclination of the stiffening is moderate, the crack penetrates the stiffening under a certain angle as defined in Fig. 11. Furthermore, the curvature of the crack paths changes at this point. Inside of the stiffening, the cracks extend steadily curved. On the backside of the stiffening, they grow towards the boundary of the stiffening. Again, the curvature of the crack paths changes where the cracks leave the stiffening. With increasing distance behind the stiffening, the crack paths approach tangentially a parallel to the extension of the initial crack. The offset of this parallel increases with rising inclination of the stiffening.

The results show that the influence of the stiffening on the deflection of the crack path depends on the orientation of the stiffening and on the stiffness mismatch of the stiffening as also shown in Fig. 15. Obviously, the effective stiffness mismatch due to a local stiffening through doubling Young´s modulus with constant thickness is greater than due to a local stiffening through doubling the thickness with constant Young´s modulus. Here it becomes noticeable, that a three dimensional FE-model is used for the crack growth simulation. Thus, particularly inside of the thickening, the stresses are not constant over the whole thickness of the specimen but the outer edges of the thickening are stress-free regions. These stress free regions do not participate in the stiffness mismatch. Therefore, obviously the effect on the crack path of a thickening with double thickness is weaker than the effect of a stiff inclusion with double Young´s modulus.
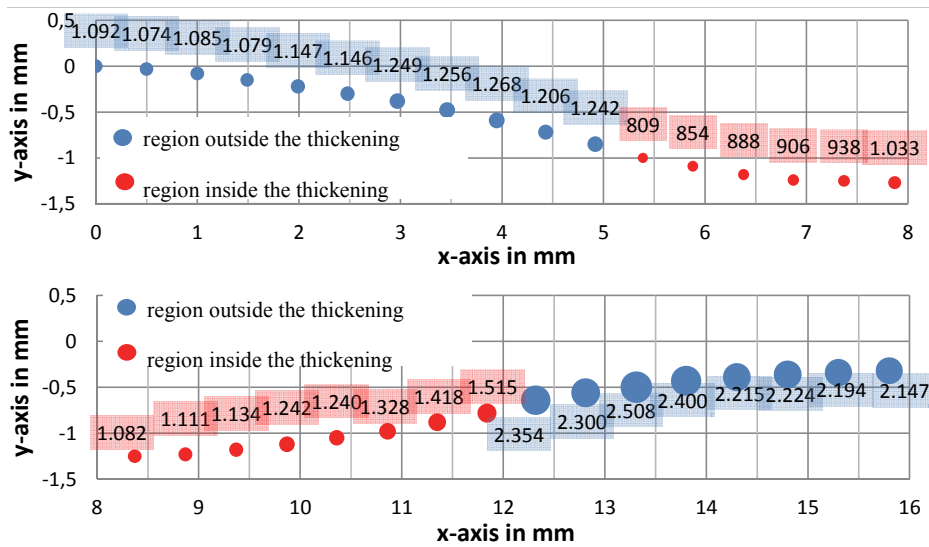
Figure 9: K_I-values along the crack path through a thickening with orientation angle α = 45°.

Fig. 9 exemplarily shows the distribution of the stress intensity factor K_I on the path through the thickening with the orientation angle α = 45° using a bubble diagram whereupon the diameter of the bubbles represents the local value of K_I. When the crack approaches the stiffening, K_I drops although the crack grows, by the reason that the stiffening causes a stress shield at the crack tip. K_I reduces about the factor $\sqrt{2}$ when the crack enters the thickening. Inside the thickening, K_I increases. When the crack exits the thickening K_I rises about the factor $\sqrt{2}$. If in contrast an inclusion with double Young´s modulus causes the stiffening then K_I rises about the factor $\sqrt{2}$ when the cracks enters the inclusion and K_I reduces about the factor $\sqrt{2}$ when crack exits the inclusion [5, 6]. Since the relations for the stress intensity factor $K_I = \sqrt{G_I E}$ and for the energy release rate $G_I = -dU/dA$, which is the energy release –dU over the increment of the crack surface dA, are valid and since with every section crossing the thickness or Young´s modulus rise or reduce by the factor 2, obviously, the energy release is continuous when the crack crosses the boundaries of the stiffening.

The evaluation of the stress intensity factor K_{II} yields that the values of K_{II} are overall small compared to the values of K_I. The greatest values of K_{II} occur, where the stiffening causes the greatest local stiffness asymmetry. At the boundaries of the stiffening, the course of K_{II} shows a zero crossing and the sign of K_{II} changes, so that at these points, the crack path has inflexion points and locally mode I-loading exists.

CRACK PATHS FOR COMPLIANT CHANGES IN STIFFNESS

Fig. 10 illustrates the comparison between crack paths due to changes in stiffness with halving Young´s modulus or halving the thickness in partition P3 for the orientation angles α = 45° and α = 60°. Firstly, the cracks grow towards the change in stiffness. With increasing inclination of the change in stiffness, the deflection of the cracks rises, whereby the entrance angle according to Fig. 11 increases. At the transition point into the compliant region, the curvature of the crack paths changes. Inside of the compliant region, the crack extends steadily curved. On the backside of the compliant region, the crack paths deflect more with increasing inclination of the change in stiffness and tend to run tangential to the region boundary. If the compliant region is big enough, the crack leaves this region on the backside, whereat the curvature of the crack path changes again. With greater distance behind the compliant region, the crack paths approach tangentially a parallel to the extension of the initial crack. The offset of this parallel to the initial crack increases with rising inclination of the change in stiffness.

In contrast to the crack paths due to a stiffening through doubling Young´s modulus or doubling the thickness as shown in Fig. 8 the crack paths due to a compliant region through halving Young´s modulus or halving the thickness are rather similar. Obviously, this may be reasoned by the fact that inside a cut-out in contrast to a thickening no stress-free regions occur, so that the effective stiffness mismatches due to both methods to generate a compliant change in stiffness are similar. The characteristics of the courses of the stress intensity factors K_I and K_{II} for the compliant regions are corresponded to the characteristics of the courses of the stress intensity factors K_I and K_{II} for the stiffening.
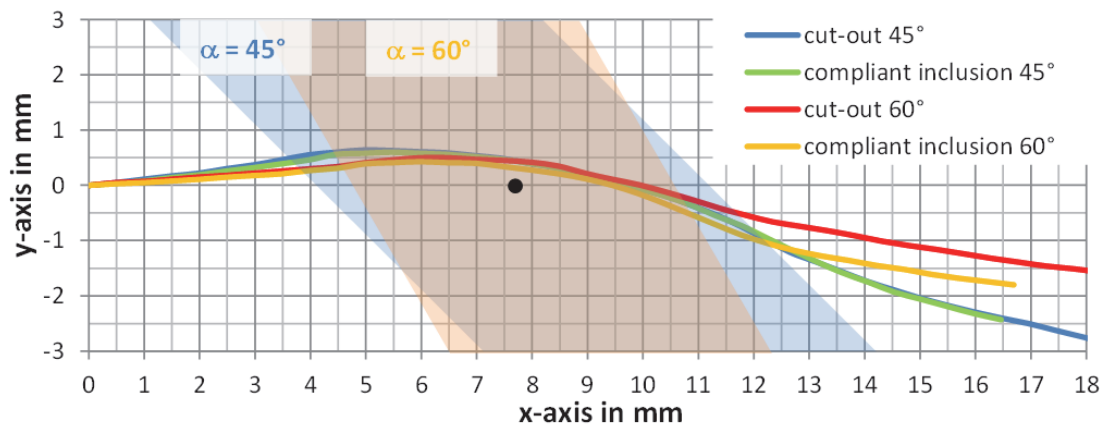
Figure 10: Crack paths for different orientation angles of compliant changes in stiffness

COMPARISON OF CRACK PATHS FOR STIFF AND COMPLIANT CHANGES IN STIFFNESS

Fig. 11 illustrates the definition of the transition angles of the crack paths at region transitions.
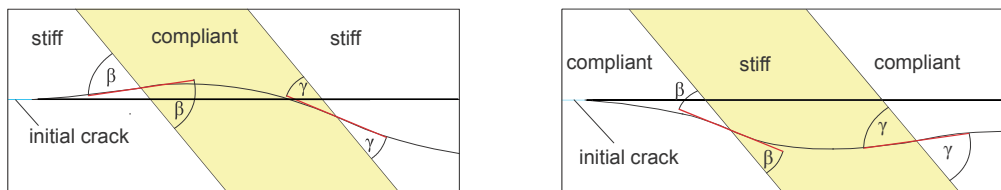

Figure 11: Definition of the entrance angle β and the exit angle γ of the crack path at region transitions.

The comparison of the transition angles in Fig. 12 and the crack paths through stiff and compliant changes in stiffness in the Figs. 7, 8 and 10 show that in both cases at the transition from a compliant to a stiff region the crack grows away from the region boundary. Therefore, the transition angle from compliant to stiff according to the definition of the transition angles in Fig. 11 becomes smaller than the orientation angle of the change in stiffness. At the transition from a stiff to a compliant region, the crack grows towards the region boundary and the transition angle becomes greater than the orientation angle of the change in stiffness. Furthermore, Fig. 12 indicates that the transition angles are equal at transitions with the same stiffness mismatch independent of what causes the change in stiffness.
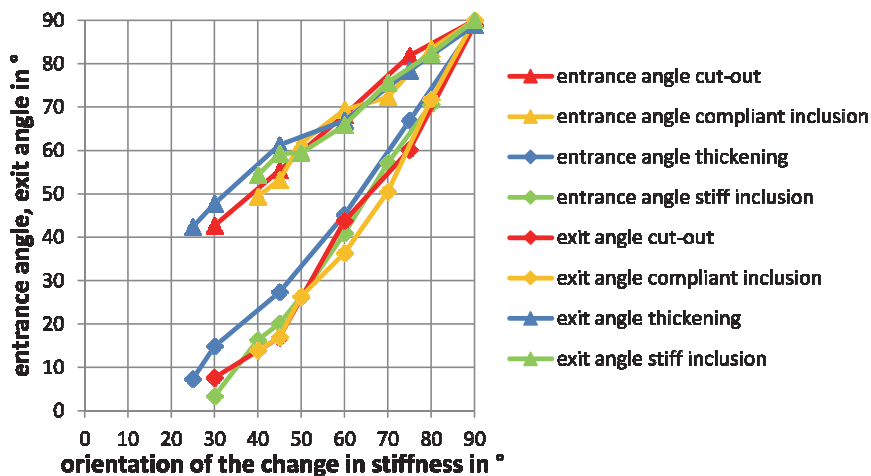

Figure 12: Comparison of the entrance and the exit angles depending on the type of the change in stiffness

CRACK PATHS DEPENDING ON THE DISTANCE OF THE CHANGE IN STIFFNESS FROM THE STARTER NOTCH

The crack paths for a stiff inclusion and a compliant inclusion with constant orientation angle α = 45° and varying distance to the starter notch are represented in Fig. 13. The distance varies in steps of 2.5mm from 9.7mm to 19.7mm.
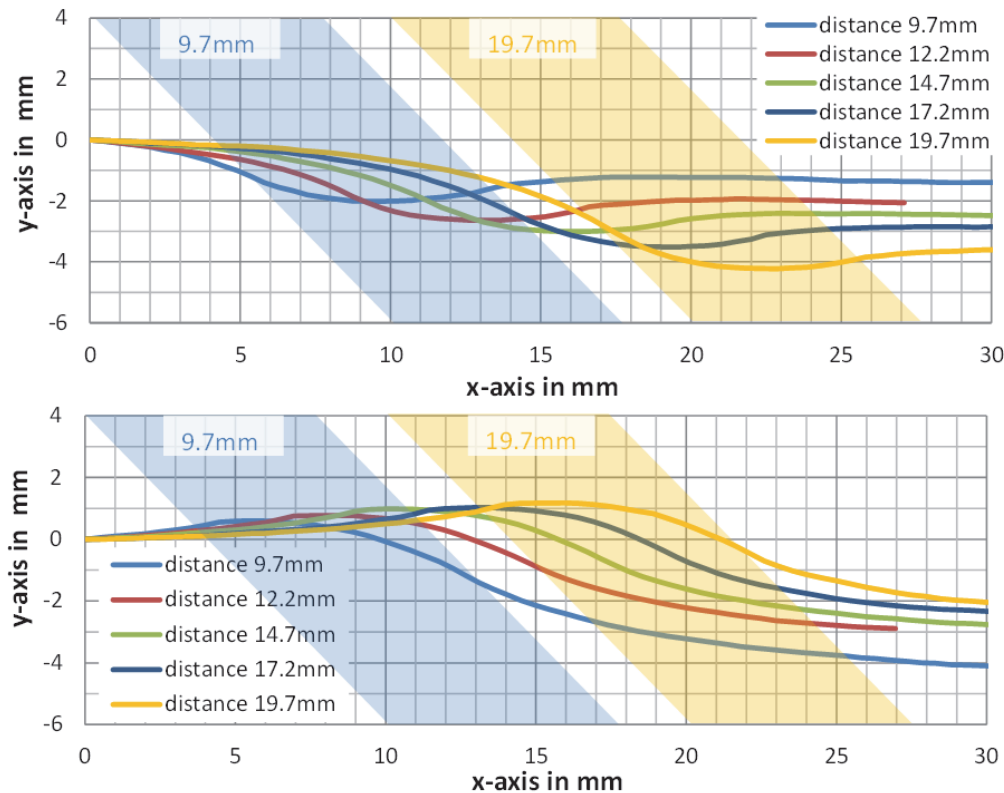

Figure 13: Crack paths for stiff inclusions (top image) and compliant inclusions (lower image) with constant orientation angle α = 45° and varying distance from the starter notch

As shown in Fig. 13 the characteristics of the particular crack paths for the stiff inclusions and the compliant inclusions are equal. In the region of influence of the inclusion, the crack deflects and the deviation of the crack path from the initial crack increases with the distance from the starter notch. Behind the inclusion, the crack grows parallel to the initial crack with a certain offset. The parallel offset behind the stiff inclusion is the bigger the greater the distance of the inclusion from the starter notch. Whereas, the parallel offset behind the compliant inclusion is the smaller the greater the distance of the inclusion from the starter notch. Superposing the crack paths, so that the entry points and the exit points coincide, shows that the crack paths through the inclusions and the transition angles according to Fig. 11 are independent of the distance of the inclusion from the initial crack but dependent on the stiffness mismatch. This is represented exemplarily in Fig. 14 for crack paths through the compliant inclusions.

The dependence of the transition angles on the stiffness mismatch represents Fig. 15. Here the transition angles for an inclusion with constant distance d = 14.7mm from the starter notch and constant orientation angle α = 45° and varying Young´s modulus are plotted over the stiffness mismatch. The stiffness mismatch Ē is defined as follows:

$$\overline{E} = \frac{E_I - E_D}{E_I + E_D} \tag{3}$$

Whereat E_I is Young´s modulus of the inclusion and E_D is the default Young´s modulus. If E_I and E_D are equal the stiffness mismatch is zero. Therefore, the crack does not deflect and the transition angles are equal to the orientation angle. If E_I is less than E_D the stiffness mismatch Ē is negative but at least -1. If E_I is greater than E_D the stiffness mismatch Ē is positive but not more than +1. The course of the entrance angle and the course of the exit angle over Ē show a counter similar behaviour. If Ē is less than a critical negative value, the entrance angle reaches a constant value and

the exit angle is zero. This means that a crack enters a sufficiently compliant inclusion but does not leave it. If Ē is greater than a critical positive value, the exit angle reaches a constant value and the entrance angle is zero. This means that a crack does not enter a sufficiently stiff inclusion. Obviously, both critical values of Ē have the same absolute value and only if Ē is within this range, the crack is able to cross the inclusion.
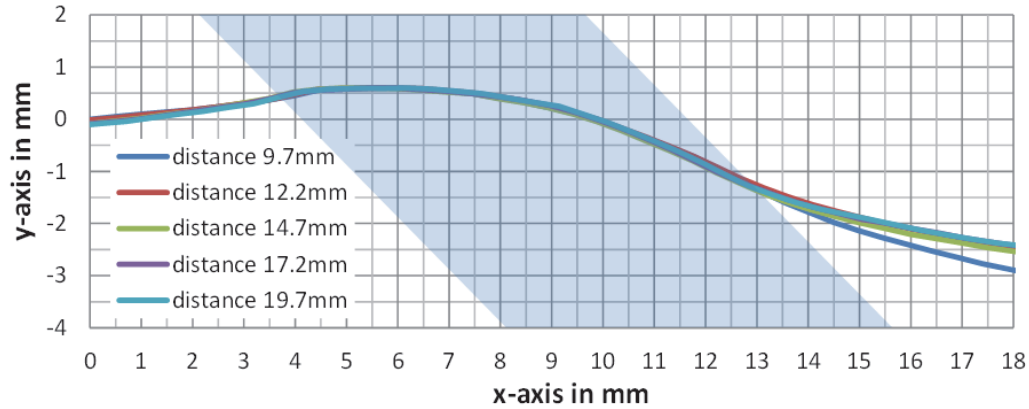

Figure 14: Comparison of the crack paths through the compliant inclusions with constant orientation angle α = 45° and varying distance from the initial crack.

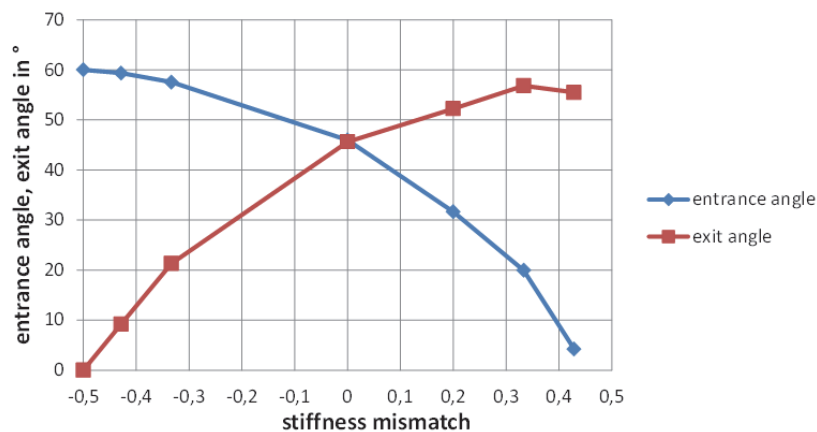Figure 15: Transition angles of cracks through inclusions with varying stiffness mismatch (α = 45°, d = 14.7mm)

CONCLUSIONS

The results of the presented investigations on the influence of changes in stiffness on the paths of fatigue cracks show, that changes in stiffness cause curved crack paths when they generate an asymmetric stiffness distribution in the neighbourhood of the crack. The deflection of the crack paths and therefore the transition angles at changes in stiffness depend on the stiffness mismatch and the orientation angle between the initial crack and the change in stiffness but they are independent on the distance between the initial crack and the change in stiffness. Only if the magnitude of the stiffness mismatch is less than a critical value the crack is able to cross the change in stiffness. Where the crack crosses the boundary of a change in stiffness the energy release is continuous and the crack path has an inflexion point.

REFERENCES

[1] Richard, H. A., Sander, M., Ermüdungsrisse, Vieweg+Teubner Verlag, Wiesbaden, (2009).
[2] Fulland M., Risssimulationen in dreidimensionalen Strukturen mit automatischer adaptiver Finite-Elemente-Netzgenerierung, Fortschritt-Bericht VDI, Reihe 18: Mechanik/Bruchmechanik Nr. 280, VDI-Verlag, Düsseldorf, (2003).

[3] Rybicki, E. F., Kanninen, M. F., A Finite Element Calculation of Stress Intensity Factors by a modified Crack Closure Integral, Engineering Fracture Mechanics, 9 (1977) 931-938.

[4] Erdogan, F., Sih, G.C., On the crack extension in plates under plane loading and transverse shear, Journal of Basic Engineering, 85 (1963) 519-525.

[5] Kullmer, G., Schramm, B., Richard, H.A., Einfluss linienförmiger Fremdeinschlüsse mit variabler Orientierung und unterschiedlichen Elastizitätsmodulen auf den Verlauf von Ermüdungsrissen. in: DVM-Bericht 246, Bruchmechanische Werkstoff- und Bauteilbewertung: Beanspruchungsanalyse, Prüfmethoden und Anwendungen, Deutscher Verband für Materialforschung und -prüfung e.V., Berlin, (2014) 73-82.

[6] Kullmer, G., Schramm, B., Richard, H.A., About the influence of line-shaped inclusions on the path of fatigue cracks, Procedia Materials Science, 3 (2014) 110-115.